International Journal of Control and Automation
Vol. 9, No. 11 (2016), pp.271-282
http//dx.doi.org/10.14257/ijca.2016.9.11.23

Induced Magnetic Field Computation for Ships Based on Fast Multipole Method and Integral Equation Method

Bian Qiang, Wang Xiang-Jun, Zhou Guo-Hua, Tong Yu-De and Liu Sheng-Dao

College of Electrical Engineering, Naval University of Engineering, China,
tzbianqiang@163.com;

Abstract

The nonsymmetric and dense coefficient matrix of integral equation method results in low computation efficiency and large memory cost in induced magnetic field computation of large scale ships. In order to improve the computation efficiency, a new method called FMMIEM is developed based on fast multipole method and integral equation method. The basic formulas of the FMMIEM were deduced. The numerical implementations of the multipole expansion, multipole to local translation and local expansion were described in detail. The FMMIEM not only has the virtue of the vector integral equation method which needs only meshing source area and is easy to deal with the infinite domain problems, such as the induced magnetic field modeling, but also has the excellent performance of the fast multipole method in conjunction with iterative solver which can accelerate the matrix vector product. The analytical numerical experiment of the sphere magnetized in the uniform applied magnetic field and the magnetostatic field modeling of the main cabin of the simple submarine mockup were designed and the results showed that the FMMIEM is with the high calculation accuracy and reduces costing time obviously. The proposed method is very helpful in engineering.

Keywords*: Integral equation method, fast multipole method, induced magnetic field computation, ship degaussing*

1. Introduction

For securing naval vessels from magnetic mines and magnetic anomaly detection equipments, it is crucial to predict the ferromagnetic signature of surface ships and submarines [1]. The ferromagnetic signature around naval vessels mainly consists of the induced magnetic field and the remanent one. Because the induced magnetic field is very important to optimize the performance of onboard signature reduction systems during their design phase, a wide interest always arise in the modeling of the induced magnetism of ferromagnetic naval vessels [2-6]. Different models for predicting the induced magnetic field were developed, such as finite element method (FEM) [7], boundary element method (BEM) [8] and integral equation method (IEM). Recently, IEM models are mostly used to predict the induced magnetic field because it is easier to deal with the open area problems and only need to mesh the source area [9-13]. However, its nonsymmetric and dense coefficient matrix results in low computation efficiency and large memory cost, which has been a serious problem for analyzing large-scale problems.

In the mid-1980s, Rokhlin and Greengard pioneered the innovative fast multipole method (FMM) that can be used to accelerate the solutions by fast matrix vector products. So a new method called FMMIEM is developed based on FMM and IEM. The proposed method can overcome the above-mentioned disadvantage and its numerical implementation was described in detail.

The organization of the paper is as follows. In section 2, vector integral equation method based on irregular hexahedron was introduced. In section 3, the numerical implementations of the multipole expansion, multipole to local translation and local

ISSN: 2005-4297 IJCA

expansion were described in detail in coupling vector integral equation method with fast multipole method. Then section 4 provides the analytical numerical experiment of the sphere magnetized in the uniform applied magnetic field and the magnetostatic field modeling of the simple submarine mockup, which are shown to verify the proposed method. Finally, section 5 concludes this paper.

2. Vector Integral Equation Method

As shown in Figure 1, according to integral equation method, when a naval vessel is placed in geomagnetic field, the induced magnetic flux density $\boldsymbol{B}$ at arbitrary filed point P around the naval vessel can be expressed as [14]

$$\boldsymbol{B}(P) = -\frac{\mu_0}{4\pi}\nabla_P \int_v \boldsymbol{M} \cdot \nabla_Q \left(\frac{1}{|\boldsymbol{r}_{PQ}|}\right) \mathrm{d}v_Q \tag{1}$$

where M represents the magnetization of the naval vessel, r_{PQ} represents the vector from the source point Q to the field point P, μ_0 represents the permeability of free space, ∇_P and ∇_Q are the gradient operator to the field coordinate and the source coordinate respectively, v is the volume of the naval vessel.

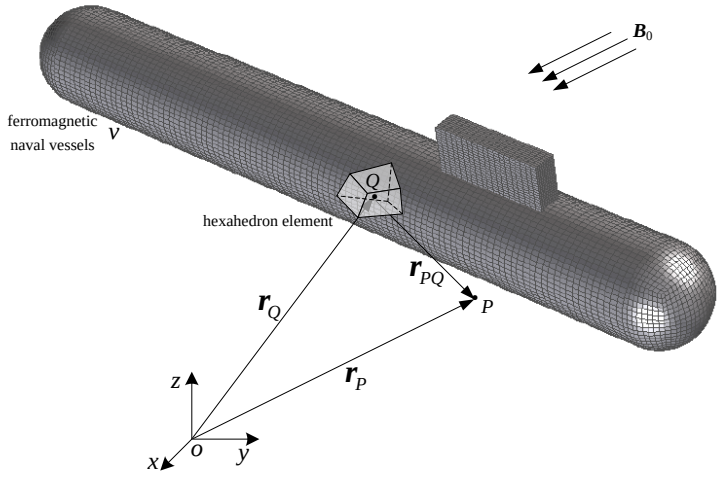

Figure 1. The Sketch Map of Magnetostatic Computation

To calculate the induced magnetic flux density $\boldsymbol{B}$ created by the naval vessel, the naval vessel should be discretized into N elements, such as irregular hexahedron elements. As far as magnetization of each element is concerned, constant element, linear element and higher-order element could be applied. For simplicity, constant element is chosen in this computation. Then Equation (1) can be simplified as

$$\boldsymbol{B}(P) = -\frac{\mu_0}{4\pi}\sum_{i=1}^{N}\left(\nabla_P \int_{s_i} \frac{\boldsymbol{M}_i \boldsymbol{n}_i}{|\boldsymbol{r}_{PQ}|}\mathrm{d}s_Q\right) \tag{2}$$

where s_i is the surface of the i^{th} hexahedron element, $\boldsymbol{n}_i$ is the outward normal of the surface s_i, N is the number of the hexahedron elements. Considering the relationship $\boldsymbol{M}=\boldsymbol{B}(\mu_r-1)/\mu_r$ and placing each of the N field points at the center of the corresponding hexahedron element, we can obtain the following system

$$\frac{\mu_{rj}}{4\pi}\sum_{i=1}^{N}\frac{\mu_{ri}-1}{\mu_{ri}}\iint_{s_i}(\boldsymbol{B}(\boldsymbol{r}_{Q_i})\cdot\boldsymbol{n}_i)\frac{\boldsymbol{r}_{P_jQ_i}}{|\boldsymbol{r}_{P_jQ_i}|^3}\mathrm{d}s_Q - \boldsymbol{B}(\boldsymbol{r}_{P_j}) = -\mu_{rj}\boldsymbol{B}_0(\boldsymbol{r}_{P_j}) \quad (j=1,2,\ldots,N) \tag{3}$$

where μ_{ri} denotes the relative permeability of each hexahedron element. Compared with other strong field, the geomagnetic field is so weak that we can

think the relative permeability μ_r is constant. Equation (3) can be transformed in matrix form as follows

$$\boldsymbol{C}_{3N\times 3N}\boldsymbol{X}_{3N}=\boldsymbol{Y}_{3N} \tag{4}$$

where C denotes a 3N×3N coefficient matrix, X denotes a 3N×1 vector composed of the magnetic flux density of each hexahedron element and Y denotes a 3N×1 vector composed of the geomagnetic field affected on each hexahedron element.

By solving the above matrix system, we can obtain the magnetic flux density of each hexahedron element. And then the induced magnetic flux density $\boldsymbol{B}$ at arbitrary field point P around the naval vessel can be calculated based on Equation (2). However, as is known to all, the coefficient matrix C is nonsymmetric and dense, which results in long computation time. In order to overcome the disadvantage, a new method called FMMIEM is developed based on FMM and IEM. The numerical implementation of the proposed method was described in detail in the following part.

3. Fast Matrix Vector Products with FMM

The main idea of the FMM is to apply iterative solvers (*e.g.,* GMRES) to solve Equation (4) and use the FMM to accelerate the matrix vector products (CX) in each iteration, without ever forming the entire matrix C explicitly. In order to achieve a fast computation of induced magnetic field created by naval vessels, we will couple FMM algorithm with vector integral equation method. The main procedure includes three parts, which is the multipole expansion (ME), moment to local translation (M2L) and local expansion (LE).

3.1. Multipole Expansion

Firstly, we should expand the kernel function to separate the field point r_P and the source point r_Q. By using spheric harmonic functions, we can obtain the following expansion [15-16]

$$\frac{1}{|\boldsymbol{r}_P-\boldsymbol{r}_Q|}=\sum_{n=0}^{\infty}\sum_{m=-n}^{n}R_{n,m}(\overrightarrow{OQ})\overline{S_{n,m}}(\overrightarrow{OP}) \qquad (|\overrightarrow{OP}|>|\overrightarrow{OQ}|) \tag{5}$$

where O is the expansion center, n denotes number of terms in multipole expansion, the overbar indicates the complex conjugate, Rnm and Snm is the two spheric harmonic functions, defined as follows

$$R_{n,m}(\overrightarrow{OQ})=\frac{1}{(\mathrm{n}+\mathrm{m})!}P_n^m(\cos\alpha)e^{im\beta}\rho^n \tag{6}$$

$$S_{n,m}(\overrightarrow{OP})=(\mathrm{n}-\mathrm{m})!P_n^m(\cos\theta)e^{im\phi}\frac{1}{r^{n+1}} \tag{7}$$

where (ρ, α, β) and (r, θ, ϕ) is the spherical coordinates of the r_Q and r_P, P_{nm} is the associated Legendre function, defined by

$$P_n^m(x)=(1-x^2)^{m/2}\frac{\mathrm{d}^m}{\mathrm{d}x^m}P_n(x) \quad (m\geq 0) \tag{8}$$

where P_n is the Legendre polynomials of degree n.

Applying Equation (5) to Equation (2), we obtain

$$\boldsymbol{B}(P)=-\frac{\mu_0}{4\pi}\sum_{i=1}^{N}(\sum_{n=0}^{\infty}\sum_{m=-n}^{n}\nabla_P\overline{S_{n,m}}(\overrightarrow{OP})M_{n,m}(O)) \tag{9}$$

where $M_{n,m}(O)$ is the multipole moment centered at O, defined by

$$M_{n,m}(O)=\int_s(\boldsymbol{M}\square\boldsymbol{n})R_{n,m}(\overrightarrow{OQ})\mathrm{d}s_Q \tag{10}$$

The procedure given by (10) is called ME. It is usually too complex to calculate Mn,m(O) analytically. Instead, $M_{n,m}(O)$ is calculated numerically using Gauss numerical integral. The relationship of each symbol in kernel function of Equation (2) is depicted in

Figure 2(a). To calculate the multipole moment $M_{n,m}(O)$, global coordinate system, isoparametric coordinate system and local coordinate system on the surface of hexahedron element are introduced. The Gauss integral points in the above coordinate systems are depicted in Figure 2(b-d) respectively. Then $M_{n,m}(O)$ can be calculated numerically by

$$M_{n,m}(O)=\sum_{i=1}^{6}\{(\boldsymbol{B}\ (Q)\square\boldsymbol{n}_i)\sum_{j=1}^{Nt}[R_{n,m}(\overrightarrow{OQ_j})\omega_j S_i]\} \qquad (11)$$

where wj is the j_{th} weight corresponding to the j_{th} integral point, N_t denotes the number of Gauss integral points and four Gauss integral points are employed here.

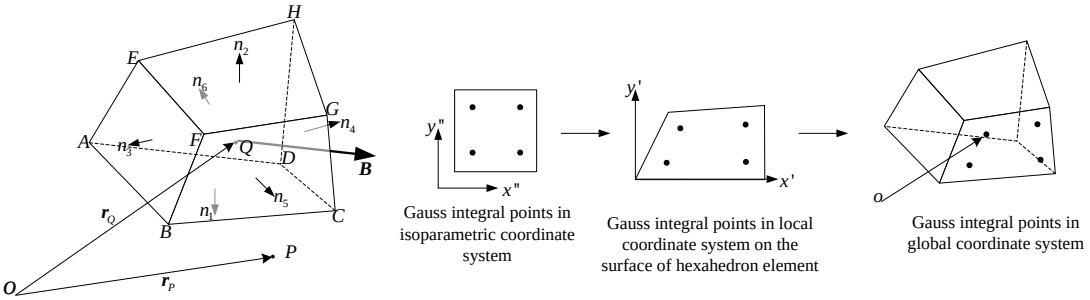

Figure 2. The Relationship of Each Symbol In Kernel Function and Gauss Integral Points In Different Coordinate Systems

3.2. Moment to Local Translation

In Figure 3, if the inequality $|\overrightarrow{OP_O}|>|\overrightarrow{P_OP}|$ holds, applying the following equation [15]

$$\overline{S_{n,m}}(\overrightarrow{OP})=\sum_{n'=0}^{\infty}\sum_{m'=-n'}^{n'}(-1)^{n'}R_{n',m'}(\overrightarrow{P_OP})\overline{S_{n+n',m+m'}}(\overrightarrow{OP_O}) \qquad (12)$$

to Equation (9), we can obtain

$$\begin{aligned}\boldsymbol{B}(P)&=-\frac{\mu_0}{4\pi}\sum_{n'=0}^{\infty}\sum_{m'=-n'}^{n'}\nabla_P R_{n',m'}(\overrightarrow{P_OP})\\&\sum_{n=0}^{\infty}\sum_{m=-n}^{n}(-1)^{n'}\overline{S_{n+n',m+m'}}(\overrightarrow{OP_O})M_{n,m}(O)\\&=-\frac{\mu_0}{4\pi}\sum_{n'=0}^{\infty}\sum_{m'=-n'}^{n'}\nabla_P R_{n',m'}(\overrightarrow{P_OP})L_{n',m'}(P_O)\\&=-\frac{\mu_0}{4\pi}\sum_{n=0}^{\infty}\sum_{m=-n}^{n}\nabla_P R_{n,m}(\overrightarrow{P_OP})L_{n,m}(P_O)\end{aligned} \qquad (13)$$

where

$$L_{n,m}(P_O)=\sum_{n'=0}^{\infty}\sum_{m'=-n'}^{n'}(-1)^{n}\overline{S_{n+n',m+m'}}(\overrightarrow{OP_O})M_{n',m'}(O) \qquad (14)$$

Apparently, Equation (14) shows us how to translate multipole moment at center O to local expansion at center PO. The procedure given by Equation (14) is called M2L translation.

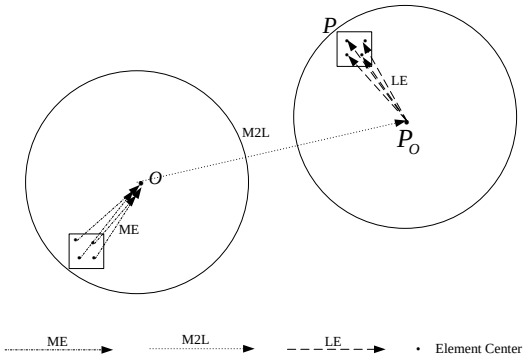

Figure 3. The Sketch Map of Multipole Expansion, Multipole to Local Translation and Local Expansion

3.3. Local Expansion

Based on Equation (13), we have

$$\boldsymbol{B}(P) = -\frac{\mu_0}{4\pi}\sum_{n=0}^{\infty}\sum_{m=-n}^{n}\nabla_P R_{n,m}(\overrightarrow{P_O P})L_{n,m}(P_O) \tag{15}$$

By applying Equation (15), we can translate local expansion at center P_O to the observe point P, which is called LE.

The above procedure refers to the gradient of the spheric harmonic functions. Fortunately, they could be calculated analytically by Equation (16) and Equation (17) [16].

$$\begin{aligned}\nabla_P S_{n,m}(\overrightarrow{OP}) &= \begin{bmatrix}\frac{\partial S_{n,m}}{\partial P_x} & \frac{\partial S_{n,m}}{\partial P_y} & \frac{\partial S_{n,m}}{\partial P_z}\end{bmatrix}^T \\ &= \begin{bmatrix}(S_{n+1,m-1} - S_{n+1,m+1})/2 \\ i(S_{n+1,m+1} + S_{n+1,m-1})/2 \\ -S_{n+1,m}\end{bmatrix}\end{aligned} \tag{16}$$

$$\begin{aligned}\nabla_P R_{n,m}(\overrightarrow{P_O P}) &= \begin{bmatrix}\frac{\partial R_{n,m}}{\partial P_x} & \frac{\partial R_{n,m}}{\partial P_y} & \frac{\partial R_{n,m}}{\partial P_z}\end{bmatrix}^T \\ &= \begin{bmatrix}(R_{n-1,m-1} - R_{n-1,m+1})/2 \\ i(R_{n-1,m-1} + R_{n-1,m+1})/2 \\ R_{n-1,m}\end{bmatrix}\end{aligned} \tag{17}$$

Obviously, the above procedure involves infinite series. Considering the balance between the computation complexity and the error caused by the truncated expansions, we choose the order of ME and LE to k=4.

3.4. Implementation Procedure of IEM Coupled with FMM

Then the implementation procedure of IEM coupled with FMM is briefly presented here.

Step 1. Discretization. Discretize the naval vessel with irregular hexahedron elements in the same manner in conventional IEM.

Step 2. Construction of octree structure. Consider a box which contains the naval vessel and call it the box of level 0. Then take a box of level l (l >0) as a parent box and divide it into eight equal sub-boxes and call any of them a child box of level l +1 if some hexahedron elements belong to this box. Stop the box subdivision if the number of

hexahedron elements belonging to the box is smaller than a given number *Nmax*. A childless box is called a leaf. In step2, five corresponding arrays are used to store the information for the octree structure of the maximum level: *itree*(*i*), which indicates the box location of the i^{th} box, *ielem*(*i*), which indicates the original hexahedron element number for the i^{th} hexahedron element, *loct*(*i*), which indicates the starting place of the hexahedron elements included in the i^{th} box in the array *ielem*, *numt*(*i*) which indicates the number of hexahedron elements included in the i^{th} box, and *ifath*(*i*) which indicates the box number of the parent box of the i^{th} box.

Step 3. Solve the Equation (4) by GMRES iterative solver. The procedure refers to a lot of matrix vector products, which can be simplified by FMM. The detailed implementation is as follows:

1) Initialize the iterative parameters and the FMM initial parameters.

2) Multipole moments computation. Firstly, we compute the multipole moments associated with leaves using Equation (11). For a non-leaf box_i of level *l*, we compute the multipole moments associated with box_i by adding all the multipole moments of box_i's children after shifting the origin from the centroids of box_i's children to that of box_i by Equation (13).

3) Coefficients computation of the local expansion during downward procedure. As far as the local expansion associated with box_i is concerned, it represents a sum of the contributions due to hexahedron elements in boxes of the interaction list of box_i and the contributions due to all hexahedron elements in boxes which are not adjacent to box_i's parent. The former is computed as we substitute the multipole moments associated with boxes in the interaction list of box_i into Equation (16) and the latter by translating the local expansion associated with box_i's parent by Equation (18). We should repeat the above procedure starting from $l = 2$ and increasing *l* along the tree structure until we reach leaves.

4) Integral evaluation in Equation (1). Considering that box_i is a box of the level *l* to which the collocation point *P* belongs, and box_j is adjacent to box_i at same level. We compute the contribution from hexahedron elements in box_j to the integral in Equation (1) at collocation points in box_i directly if either box_i or box_j is a leaf, or else, do downward procedure by increase *l*. When box_i is a leaf, we also compute the right side of Equation (15) using the coefficients of the local expansion associated with box_i. The sum of all these terms as *l* increases from 2 gives the integral in Equation (1) evaluated at the collocation points of all hexahedron elements.

5) Update the magnetic flux density by GMRES.

Step 4. If either the error criterion or the maximum iterative time is satisfied, exit the solver. Or else go back to 2) in step3.

The above procedure of IEM coupled with FMM is programmed based on Fortran90 and tested on PC with 3.4GHz CPU and 4GB RAM. Figure 4 shows the flow chart of IEM coupled with FMM.

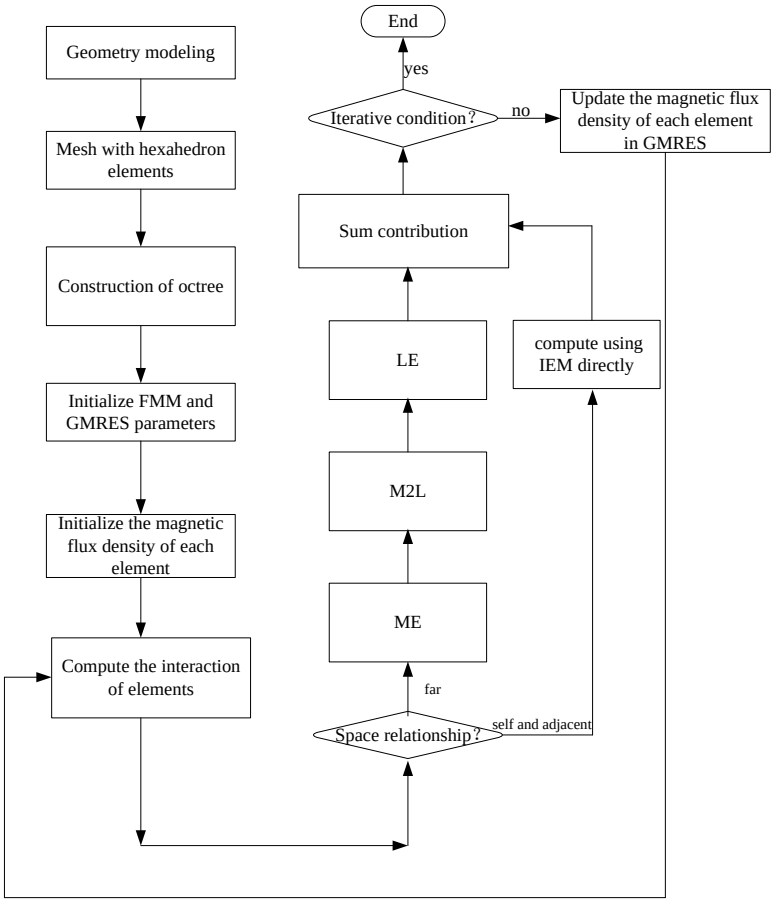

Figure 4. The Flow Chart of IEM Coupled With FMM

4. Experiments and Results

Two examples are shown to verify the proposed algorithm, one is analytical numerical example, that is the induced field computation of the sphere immerged into the uniform external magnetic field; the other is the magnetostatic field modeling of the simple submarine mock-up immerged into geomagnetic field.

4.1. Analytical Numerical Example

An iron sphere with radius 10m and relative permeability 150 is immerged into an external uniform field $\boldsymbol{B}_0$=34500$\boldsymbol{e}_x$nT. In computation of the induced field caused by iron sphere, 61 spots is arranged along with x axis equally (shown in Figure 5). We can get the analytical solution in Ref.[11], which will be compared with the calculated field by the proposed algorithm. The iron sphere is discretized with 729, 1331, 1728, 2197 and 3375 irregular hexahedron elements respectively. In each mesh condition, the induced field at all spots is calculated using both conventional IEM [11] and the proposed algorithm. The maximum hexahedron elements number *Nmax* in each box is set as $\sqrt{EleNum}$ [17], where *EleNum* is number of hexahedron elements. The maximum error and the maximum time in GMRES is set as 10^{-8} and 50 respectively.

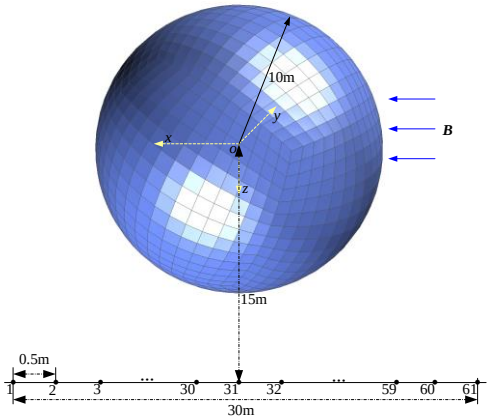

Figure 5. The Mesh of the Iron Sphere Submerged In An External Magnetic Field

Figure 6 shows the curves of analytical induced field (labeled as Theory), calculated one by conventional IEM (labeled as DIEM) and by proposed algorithm (labeled as FMMIEM) under mesh with 729 hexahedron elements. Bx, By and Bz denote the X component, Y component and Z component of the induced field respectively. Figure 7 show the computation time of the two numerical methods.

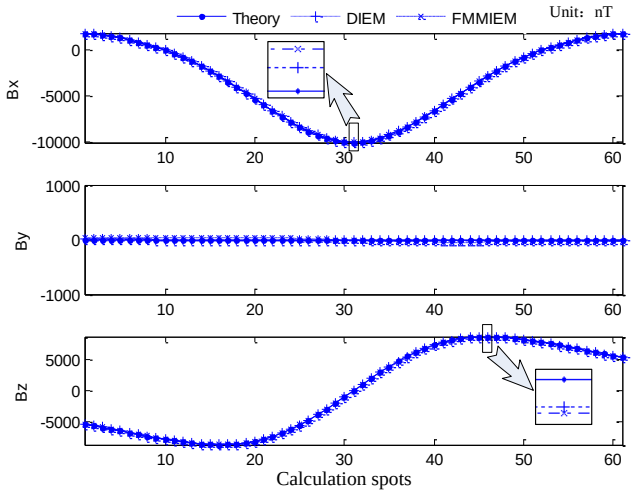

Figure 6. The Comparison of the Calculated Induced Field and the Analytical One

As is shown in Figure 6, compared with the analytical induced field, the computation error of the conventional IEM and the proposed algorithm is with 0.49% and 0.63% respectively, both are satisfying. The latter error is little greater than the former, which is caused by the contribution of elements far away calculated approximately by FMM. As is shown in Figure 7, if the conventional IEM is coupled with FMM, the performance in computation time can be greatly improved, which is very satisfying.

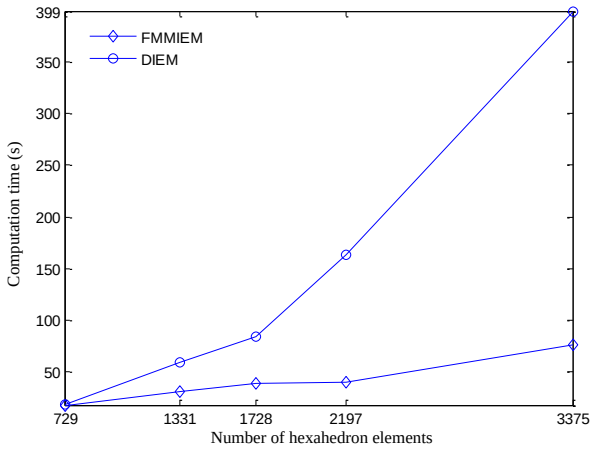

Figure 7. The Comparison of the Computation Time of the Two Numerical Methods

4.2. Mock-up Experiment

A simplified submarine mock-up with relative permeability 100~300, length 2008mm, outer radii 300mm and thickness 6mm is submerged in a geomagnetic field with horizontal component 34500nT and vertical component 34800nT. 93 filed points are arranged in three lines located under larboard, keel and starboard respectively, shown in Figure 9. In the laboratory, the mock-up is placed on the nonmagnetic carrier on a track. Three magnetic sensors are placed under the track in a line vertical to the track. When the nonmagnetic carrier moves on the sensors, the magnetic anomaly of the mock-up can be recorded. To eliminate the influence of the permanent magnetization, the mock-up is placed in four different courses when measuring. Based on the measured field in four courses, we can obtain the measured induced field, which is used to compare with the calculated field.

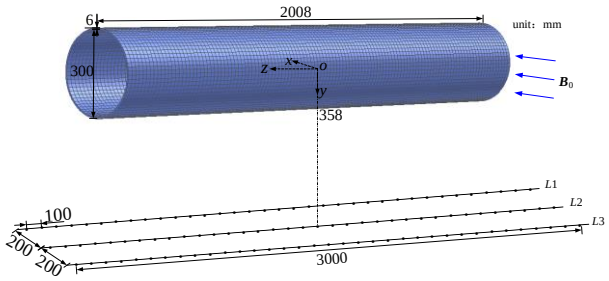

Figure 8. The Experiment Sketch Map of Tthe Simplified Submarine Mockup Submerged In Geomagentic Field

In computation of the induced field, the mock-up is discretized with 8160 irregular hexahedron elements. The maximum number of hexahedron elements *Nmax* in each box is set as $\sqrt{EleNum}$. The iterative parameters in GMRES are the same as the sphere numerical example. It takes more than one hour to calculate the induced field using conventional IEM. However, only 214 seconds are cost when using FMMIEM. Figure 10 shows the curves of the measured induced field and the calculated field created by the mock-up. The induced field data is normalized. As shown in Figure 10, the calculated induced field shows good agreement with the measured one and the maximum relative

error is 4.14%.

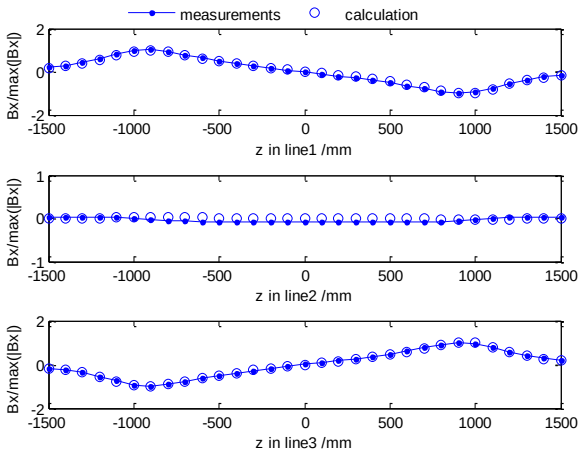

Figure 9. The Comparison of the Calculated Induced Field and the Measured One of the Simplified Submarine Mockup

5. Conclusion

In this paper, we have developed an approach for a fast computation of induced magnetic field created by naval vessels, which can overcome the disvantage of the conventinal IEM with low computation efficiency. The results of the sphere numerical example and the simplified submarine mock-up experiment show that its accuracy is satisfying and the computaiton time could be greatly improved. In addition, the proposed algorithm could also be applied in magnetic anomaly modeling for other ferromagnetic objects.

Acknowledgment

This work is supported in part by National Natural Science Foundation of China under grant No. 51107145, No. 51377165 and No. 61203193.

References

[1] A.V. Kildishev, R. Kamondetdacha and J.A. Nyenhuis, "Prediction of the Magnetic Field Below an Axisymmetrical Planar Sensor Array with a Magnetic Source Located above the Measurement Plane", Digest of Technical Papers, **(2002)**, DT9.
[2] O. Chadebec, J. Coulomb and J. Bongiraud, "Recent Improvements for Solving Inverse Magnetostatic Problem Applied to Thin Shells", IEEE Trans. Magnetics, vol. 38, no. 2, **(2002)**, pp. 1970-1975.
[3] R. Kamondetdacha, A. V. Kildishev and J. A. Nyenhuis, "Multipole Characterization of a Magnetic Source Using a Truncated SVD", IEEE Trans. Magnetics, vol. 40, no. 4, **(2004)**, pp. 2176-2178.
[4] Z. Guohua, X. Changhan and L. Shengdao, "Inversion Approach to Predicting the Magnetic Field Distribution Based on Planar Field Measurements", International Journal of Applied Electromagnetics and Mechanics, vol. 33, no. 3-4, **(2010)**, pp. 1033-1040.
[5] X. Brunotte, G. Meunier and J. Bongiraud, "Ship Magnetizations Modeling by the Finite Element Method", IEEE Trans. on Magnetics, vol. 29, no. 2, **(1993)**, pp. 1970-1975.
[6] F. Damidau, B. Bandelier and P. Penven, "A Fast and Precise Determination of the Static Magnetic Field in the Presence of Thin Iron Shells", IEEE Trans. Magnetics, vol. 31, no. 6, **(1995)**, pp. 3491-3493.
[7] O. Chadebec, J L Coulomb and V. Leconte, "Modeling of static magnetic anomaly created by iron plates", IEEE Trans. Magn, vol. 36, no. 4, **(2000)**, pp. 667-671.
[8] Y. Vuillermet, O. Chadebec and J. L. Coulomb, "Scalar Potential Formulation and Inverse Problem Applied to Thin Magnetic Sheets", IEEE Trans. Magnetics, vol. 44, no. 6, **(2008)**, pp. 1054-1057.

[9] Z. Guohua, X. Changhan and L. Shengdao, "3D magnetostatic field computation with hexahedral surface integral equation method", Tansactions of China Electrotechnical Society, vol. 24, no. 3, **(2009)**, pp. 1-7.
[10] C. Jie and L. Xiwen, "A new method for predicting the induced magnetic field of naval vessels", Acta Physica Sinica, vol. 59, no. 1, **(2010)**, pp. 239-245.
[11] T.-S. Nguyen, J.-M. Guichon and O. Chadebec, "Ships Magnetic Anomaly Computation With Integral Equation and Fast Multipole Method", IEEE Trans. Magn, vol. 47, no. 5, **(2011)**, pp. 1414-1417.
[12] J. J. Holmes, "Exploitation of A Ship's Magnetic Field Signatures", Morgan & Claypool Publishers, **(2006)**.
[13] F. Mingwu and Y. Weili, "Integral Equation Method in Electromagnetics", Beijin: China Machine Press, **(1998)**.
[14] K. Yoshida, "Application of Fast Multipole Method to Boundary Integral Equation Method", Japan: Kyoto Univ. Press. **(2001)**.
[15] L. Yi-jun, "Fast multipole boundary element method theory and applications in engineering", New York: Cambridge University Press, **(2009)**.
[16] S. Xinqing, "Gist of Electromagnetic Computation", Beijing: Science Press, **(2004)**.

Authors

Bian Qiang, he is a Lecturer, received the B.Eng. degree from the Electronic Engineering, Naval University of Engineering, wuhan, China, in 2000 and the M. Eng. degree from the System Engineering, Naval University of Engineering in 2008. He is currently working towards the Ph.D. at the school of Electronic Engineering, Naval University of Engineering, China. He has published more than 20 technical journal papers and international conference papers. He mainly engaged in the research of ship degaussing technology.